Realistic microscopic approach to deep inelastic scattering of electrons off few-nucleon systems

C. Ciofi degli Atti
Department of Physics, University of Perugia, Via A. Pascoli, I-06100 Perugia, Italy
and Istituto Nazionale di Fisica Nucleare, Sezione Sanità, Viale Regina Elena 299, I-00161 Roma, Italy

S. Liuti
Istituto Nazionale di Fisica Nucleare, Sezione Sanità, Viale Regina Elena 299, I-00161 Roma, Italy
(Received 28 August 1989)

The contribution of the nucleonic component to deep inelastic lepton scattering off ^{2}H, ^{3}H, ^{3}He, and ^{4}He nuclei is analyzed in terms of momentum distributions and spectral functions obtained from few-body calculations which employ realistic nucleon-nucleon interactions. The nuclear structure function is evaluated within the framework of the convolution model taking relativistic effects into account by means of the flux factor. A comparison with previous calculations performed with a nonrelativistic normalization of the spectral function and using, in the case of ^{4}He, an independent particle model, is presented. It is shown that short-range and tensor correlations resulting from realistic nucleon-nucleon interactions strongly increase the nucleon mean removal and kinetic energies and, consequently, enhance the calculated European Muon Collaboration effect in the direction suggested by the experimental data in the region $0.2 \leq x \leq 0.7$; for $x \leq 0.2$ and $x \geq 0.7$, an appreciable discrepancy between theory and experiment still persists and the difficulties in giving an interpretation of the effect in the whole range of x, in terms of nucleonic degrees of freedom only, are pointed out. The role of Q^2 rescaling is analyzed; it is found that present experimental data seem to require only a small increase of the quark confinement size for a nucleon imbedded in the nuclear medium. The nuclear structure function for three-nucleon systems is calculated in the region $x > 1$, where it is shown to be very sensitive to the correlation structure of the nucleon spectral function.

I. INTRODUCTION

The role played by nucleonic degrees of freedom in deep inelastic scattering (DIS) of leptons by nuclei has been widely discussed for many years (see, e.g., Ref. 1). With the experimental measurement of the quantity $R_A(x,Q^2)$, which represents the ratio of the nuclear structure function per nucleon $F_2^A(x,Q^2)$ to the deuteron one $F_2^D(x,Q^2)$, this role became the object of intensive discussions. In fact, if, as naively expected, the nucleus behaves as a collection of A free incoherent scattering centers, $R_A(x,Q^2)$ should be equal to one for all values of Bjorken's variable x, in disagreement with the experimental observations [European Muon Collaboration (EMC) effect][2-5] which show deviations from unity up to 20% in the range $0 \leq x \leq 1$.

Owing to the fact that the consideration of nucleon dynamics by simply taking into account the nucleon momentum distribution (Fermi motion) produced a very small deviation of $R_A(x,Q^2)$ from unity,[1,6] a series of calculations have been performed based upon nuclear exotic effects, such as the excess of pions per nucleon,[7] the enlargement of quark confinement radii due to the presence of six-quark components in the nuclear wave function,[8] and other effects (for a review see, e.g., Ref. 9). More recently, the interest in the contribution of nucleonic degrees of freedom to the EMC effect has been renewed, thanks to the papers by Akulinichev *et al.*[10] (see also Refs. 11 and 12), who have demonstrated that the nucleon binding (or, better, the nucleon removal energy E) plays an important role in DIS. By using a single-particle (s.p.) description in which the target nucleons occupy states α below the Fermi level, each of them characterized by a s.p. momentum distribution $n_\alpha(k)$ and s.p. energy ε_α (with $E = |\varepsilon_\alpha|$), it was indeed possible in Refs. 10–12 to explain the experimental behavior of $R_A(x,Q^2)$, whose deviation from unity turned out to be essentially governed by the average value of the removal energy $\langle E \rangle$. Frankfurt and Strikman,[13] however, have argued that when relativistic effects are consistently taken into account by considering the so-called flux factor in the normalization of the relativistic spectral function, the contribution of nucleonic degrees of freedom to the EMC effect should be strongly reduced (the necessity of properly considering the flux factor has also been stressed in Refs. 14–17). It has indeed been shown in Ref. 18 that when the flux factor is considered, the quantity $R_A(x,Q^2)$ calculated within the s.p. Hartree-Fock picture of the nucleus, exhibits only a very small deviation from unity. The use of a s.p. description of DIS has, however, been questioned in Ref. 19, where it has been shown that nucleon-nucleon (NN) correlations induced by realistic interactions, by generating high virtual excited components in the ground-state wave function [mainly two-particle-two-hole (2p-2h) excitations], strongly increase the average value of the removal energy $\langle E \rangle$, and therefore lead to an enhancement of the EMC effect.

When the effects of ground-state correlations are considered in DIS, the electron can also interact with target nucleons, which are located outside the Fermi surface

and which have high values of the momentum k and the removal energy E; as a consequence, the final $(A-1)$-nucleon system can be left in many breakup configurations (mainly 1p-2h excitations), unlike what happens in a s.p. description, in which only 1h excitations of the final system can be created. For such a reason, using in DIS a removal energy distribution (with $\langle E \rangle \approx 25-30$ MeV) taken from the "old generation" $(e,e'p)$ exclusive quasielastic experiments[20] is highly a questionable procedure because those experiments covered a narrow range of nucleon momentum and removal energy ($E \leq 60$ MeV, $k \leq 1.5$ fm^{-1}), so that only s.p. properties of nuclei could effectively be investigated. As a matter of fact, recent $(e,e'p)$ experiments[21] performed at $E \geq 60$ MeV and $k \geq 1.5$ fm^{-1} show that indeed in this region the cross section is dominated by the scattering of the electron by a correlated NN pair, in agreement with theoretical calculations of the spectral function and momentum distributions.[22] Therefore, as first pointed out in Ref. 14, in order to fully clarify the role played by conventional nuclear physics in DIS of leptons off nuclei, it is necessary to properly consider, at the same time, both the effect of the flux factor, which reduces the nucleonic contribution to the EMC effect, as well as the effect of correlations, which is expected, due to the increase of $\langle E \rangle$, to enhance it. A calculation of the EMC effect taking into account both the flux factor and the effects of correlations, has been presented in Ref. 19, where it has been shown that, even if the flux factor is considered, the enhancement produced by correlations is such that the observed deviation of $R_A(x,Q^2)$ from one can reasonably be reproduced, at least in the range $0.2 \leq x \leq 0.7$.

Calculations of Ref. 19 have been performed for complex nuclei and only the region $0 < x < 1$ has been considered. The aim of this paper is as follows: (i) to extend the approach of Ref. 19 to few-nucleon systems, ^{2}H, ^{3}He, and ^{4}He, for which the correlated momentum and removal energy distributions [i.e., the spectral function $P(k,E)$] are known with much better accuracy than for complex nuclei; (ii) to check, in this way, the approximated spectral function used for complex nuclei in Ref. 19; (iii) to calculate the nuclear structure function for $A=3$ for $x > 1$ where, unlike in the region $x < 1$, the detailed correlation structure of nuclei is expected to show up in a substantial way.

In our calculations, "exact" spectral functions for the three-body systems[22] are used, whereas for ^{4}He the model spectral function of Ref. 19, which will be shown to be a rather realistic one for $x < 1$, will be adopted.

For two- and three-nucleon systems, a calculation similar to the one presented in this paper in the region $x < 1$, has recently appeared.[23] Our work differs from Ref. 23 mainly in the following points: (i) the flux factor, disregarded in Ref. 23, is taken into account; (ii) calculations are also performed for ^{4}He for which, unlike the two- and three-body systems, good experimental data are available; (iii) the region $x > 1$ for ^{3}He is also considered.

Our paper is organized as follows. The basic assumptions leading to the convolution formula are summarized in Sec. II; the main ingredients underlying the nuclear structure function are illustrated in Sec. III; the expressions for the DIS structure functions of ^{2}H, ^{3}He, ^{3}H, and ^{4}He are given in Sec. IV; possible variations of the quark confinement radius for a bound nucleon within the Q^2-rescaling mechanism, are considered in Sec. V; the three-body structure functions for $x > 1$ is presented in Sec. VI; finally, the summary and conclusions are given in Sec. VII.

II. BASIC FORMALISM

The nucleonic contribution to the inclusive cross section for DIS of leptons off nuclei, is evaluated assuming the validity of the impulse approximation (IA) described by the Feynman diagram in Fig. 1. The main assumptions underlying the IA are (i) the nuclear hadronic tensor $W^A_{\mu\nu}$ depends only upon the one-body electromagnetic current $J^A_\mu = \sum_N J^{(N)}_\mu$, the summation being extended to the A nucleons in the nucleus; (ii) the virtual photon is scattered incoherently from the nucleons, which means that interference terms between nucleonic currents do not contribute to the cross section; (iii) the final-state interaction with the residual $A-1$ system is disregarded.

In what follows, $P_A \equiv (M_A,0)$ will denote the four momentum of the initial nucleus in the laboratory system, and $p \equiv (p_0,\mathbf{p})$ and $q \equiv (q_0,-\mathbf{q})$ the four momenta of the struck nucleon and of the virtual photon, respectively. The invariant quantities, in terms of which the convolution formula is written, are defined in terms of these four momenta as follows:

$$x = [Q^2/2(P_A q)]M_A/M_N = Q^2/2M_N\nu \,,$$

$$x' = Q^2/2(pq) \,, \tag{2.1}$$

$$z = [(pq)/(P_A q)]M_A/M_N = x/x' \,,$$

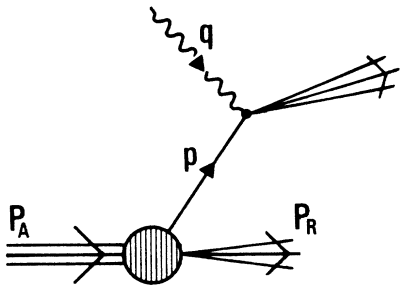

FIG. 1. The Impulse Approximation diagram for Deep Inelastic Scattering of electrons (muons) off nuclei. The relevant four momenta in the laboratory system are: $P_A \equiv (M_A,0)$, $q \equiv (q_0,-\mathbf{q})$, $p \equiv (p_0,\mathbf{p}) \equiv (M_A - \sqrt{(M^{*2}_{A-1}+\mathbf{p}^2)},\mathbf{p})$ and $P_R \equiv (\sqrt{(M^{*2}_{A-1}+\mathbf{P}^2_R)},\mathbf{P}_R)$, and refer, respectively, to the initial nucleus A, to the exchanged photon, to the struck nucleon and to the recoiling final $A-1$ system.

where $Q^2=-q^2$, $\nu\equiv q_0$, M_N is the nucleon mass, and, finally, x is the usual Bjorken variable which, in A-body nuclei, ranges from 0 to $M_A/M_N\cong A$. The kinematic region corresponding to DIS is defined by the Bjorken limit: $Q^2\to\infty$, $\nu\to\infty$, x remaining fixed; in this limit the invariant quantity z, which represents Møller's invariant flux factor in DIS cross sections, reduces (apart from the nucleon mass M_N) to the light cone component (+) of the four-momentum p:

$$z\to p^+/M_N=(p_0-p_\parallel)/M_N \ .$$

The derivation of the expression for the nuclear structure function $F_2^A(x,Q^2)$ from the diagram in Fig. 1 was at the origin of some controversy concerning the presence the flux factor z in the final convolution formula (see, e.g., Ref. 13); as a matter of fact, many calculations have omitted this factor violating in this way Lorentz invariance, as pointed out by Krzywicki[14] and Jaffe,[16] and disregarding, at the same time, important relativistic correction terms of order $\mathbf{p}^2/M_N^2$ (see Secs. III and IV).

By direct evaluation of the Feynman diagram in Fig. 1, the following convolution formula for the nuclear hadronic tensor $W_{\mu\nu}^A$ is obtained

$$W_{\mu\nu}^A=\sum_\sigma\int d^4p[(Z/A)\mathcal{S}_A^p(P_A,p,\sigma)W_{\mu\nu}^p(p,q,\sigma) +(N/A)\mathcal{S}_A^n(P_A,p,\sigma)W_{\mu\nu}^n(p,q,\sigma)] \ , \tag{2.2}$$

where Z and N are the number of protons and neutrons, respectively, $\mathcal{S}_A^{p(n)}$ is the invariant function describing the nuclear vertex with an outgoing virtual proton (p) or neutron (n) (for more details on the form and transformation properties of $\mathcal{S}_A$ see, e.g., Refs. 15 and 16), and, finally, $W_{\mu\nu}^{p(n)}$ is the hadronic tensor for the off-shell proton (neutron) with spin σ,

$$W_{\mu\nu}^{p(n)}=\{[(-g_{\mu\nu}+q_\mu q_\nu/q^2)W_1^{p(n)}(x,Q^2) +p'_\mu p'_\nu W_2^{p(n)}(x,Q^2)/M_N^2]\bar u(p,\sigma)\not{K}u(p,\sigma)\} \tag{2.3}$$

with

$$p'_\mu=p_\mu-[(pq)/q^2]q_\mu \ ,$$

and

$$\bar u(p,\sigma)\not{K}u(p,\sigma)=[\bar u(p,\sigma)\not{q}u(p,\sigma) +\bar u(p,\sigma)\not{p}u(p,\sigma)+M_N]M_N/(pq) \ . \tag{2.4}$$

In principle, the structure functions W_1 and W_2 should also depend upon the invariant p^2, i.e., on the nucleon off shellness. In the following, off-shell effects will be disregarded and the same structure functions as the free nucleon ones, with the same Q^2 and final-state mass, will be adopted.[6]

The convolution formulae for W_1 and W_2 are extracted from Eq. (2.2) by comparing appropriate linear combinations of the components of the nucleonic and nuclear hadronic tensors. For W_2 one obtains

$$W_2^A(x,Q^2)=\int d^4p\left[(Z/A)\sum_\sigma[\mathcal{S}_A^p(P_A,p,\sigma)\bar u(p,\sigma)\not{K}u(p,\sigma)](x/x')^2\mathcal{J}W_2^p(x',Q^2)+(\text{neutron term})\right] , \tag{2.5}$$

where

$$\mathcal{J}=(1+2p_\parallel x'/|\mathbf{q}|)^2+2x'^2\nu^2(\mathbf{p}^2-p_\parallel^2)/|\mathbf{q}|^2Q^2) \ . \tag{2.6}$$

By performing the Bjorken limit, the factor $\mathcal{J}$ becomes equal to one, $\not{q}\to\nu\gamma^+$, and the last two terms in Eq. (2.4) can be disregarded being of order M_N/ν; moreover, setting $W_2^{p(n)}=\nu F_2^{p(n)}$, one has

$$F_2^A(x,Q^2)=\int d^4p\left\{(Z/A)\left[\sum_\sigma\mathcal{S}_A^p(P_A,p,\sigma)\bar u(p,\sigma)\gamma^+u(p,\sigma)/z\right]zF_2^p(x/z,Q^2)+(\text{neutron term})\right\} . \tag{2.7}$$

By averaging over the spin in Eq. (2.7) and defining the light cone momentum distribution as

$$f_A^{p(n)}(z)=\int d^4p\mathcal{S}_A^{p(n)}(p)z\delta\{z-[(pq)/(P_Aq)]M_A/M_N\} \tag{2.8}$$

with

$$\mathcal{S}_A^{p(n)}(p)=\sum_\sigma\mathcal{S}_A^{p(n)}(P_A,p,\sigma) \ ,$$

the final convolution formula for the nuclear structure function is obtained as follows:

$$F_2^A(x,Q^2)=\int_{x\le z}dz[(Z/A)f_A^p(z)F_2^p(x/z,Q^2)+(N/A)f_A^n(z)F_2^n(x/z,Q^2)] \ . \tag{2.9}$$

The normalizations of

$$\mathcal{S}_A(p)=[(Z/A)\mathcal{S}_A^p(p)+(N/A)\mathcal{S}_A^n(p)] \ , \tag{2.10}$$

$$f_A(z)=[(Z/A)f_A^p(z)+(N/A)f_A^n(z)] \ , \tag{2.11}$$

are obtained from baryon number conservation, i.e., from the calculation of the Feynman diagram for the nuclear form factor using the same prescriptions adopted for the calculation of the IA diagram[13,15]

$$\int d^4p\mathcal{S}_A(p)z=\int dz\, f_A(z)=1 \ . \tag{2.12}$$

The separated contributions of protons and neutrons are

normalized according to

$$\int d^4p\,\mathcal{S}^p_A(p)z = \int dz\, f^p_A(z)=1\ , \tag{2.13}$$

$$\int d^4p\,\mathcal{S}^n_A(p)z = \int dz\, f^n_A(z)=1\ . \tag{2.14}$$

The quantity which must be compared with the experimental data is the ratio

$$R_A(x,Q^2)=\frac{F_2^A(x,Q^2)}{F_2^D(x,Q^2)}I(x,Q^2)\ , \tag{2.15}$$

where $F_2^A(x,Q^2)$ is given by Eq. (2.9) and

$$F_2^D(x,Q^2)=\int_{x\le z} dz\, f_D(z)[F_2^p(x/z,Q^2) + F_2^n(x/z,Q^2)]/2 \tag{2.16}$$

is the deuteron structure function per nucleon. The factor $I(x,Q^2)$, defined as

$$I(x,Q^2)=\frac{[F_2^p(x,Q^2)+F_2^n(x,Q^2)]/2}{[ZF_2^p(x,Q^2)+NF_2^n(x,Q^2)]/A}\ , \tag{2.17}$$

is the so-called isoscalarity correction, which ensures that when nucleon dynamics is completely disregarded [by setting $f^p_A(z)=f^n_A(z)=\delta(z-1)$], the relation $R_A(x,Q^2)=1$ is satisfied for all values of x. For isoscalar nuclei ($N=Z=A/2$, $f^p_A=f^n_A=f_A$) one has $I(x,Q^2)=1$ and

$$R_A(x,Q^2)=\frac{\int_{x\le z} f_A(z)\bar{F}_2^N(x/z,Q^2)dz}{\int_{x\le z} f_D(z)\bar{F}_2^N(x/z,Q^2)dz}\ , \tag{2.18}$$

where

$$\bar{F}_2^N(x/z,Q^2)=[F_2^p(x/z,Q^2)+F_2^n(x/z,Q^2)]/2\ . \tag{2.19}$$

From the preceding derivation of the convolution formula, it can be easily seen that the omission of the factor z, both in the definition of the nuclear structure function [Eq. (2.9)] and in the normalization of $f_A(z)$ [Eq. (2.12)], was due, in many calculations,[10–12] to the replacement, e.g., in Eq (2.7), of the matrix γ^+, with the matrix γ^0.[15–17]

Equations (2.8) and (2.9) show that the calculation of the nuclear structure function F_2^A requires the knowledge of the function $\mathcal{S}_A(p)$. In the nonrelativistic limit, the following expansion holds[13] [if, in what follows, the superscripts p and n do not appear explicitly in a given equation, the latter is meant to hold for both protons and neutrons as well as for the summed quantities with proper weights, as in Eqs. (2.10) and (2.11)]:

$$\mathcal{S}_A(p)=P(|\mathbf{p}|,E)[1+O(\mathbf{p}^2/M_N^2)+\cdots]\ , \tag{2.20}$$

where $P(|\mathbf{p}|,E)$ is the nonrelativistic spectral function (see, e.g., Ref. 24 and Sec. III), which obeys the following normalization condition:

$$\int d^3p\,dE\,P(|\mathbf{p}|,E)=1\ . \tag{2.21}$$

Equation (2.20) has been adopted in our calculations, retaining terms up to the order $\mathbf{p}^2/M_N^2$. In Ref. 23, the "*ad hoc*" assumption $z\mathcal{S}_A(p)\equiv P(|\mathbf{p}|,E)$ has been made, on the grounds that both the relativistically invariant function $z\mathcal{S}_A(p)$ and the nonrelativistic spectral function $P(|\mathbf{p}|,E)$ are normalized to unity [cf. Eqs (2.12) and (2.21)]. Such an assumption produces the same effect as disregarding the flux factor in the convolution formula [Eq. (2.9)]; as will be shown in Sec. IV, this means that relativistic corrections of order $\mathbf{p}^2/M_N^2$, which largely reduce the value of the ratio $R_A(x,Q^2)$ for $0.2\le x\le 0.7$, are not taken into account.

In conclusion, the calculation of the nucleonic contribution to the full nuclear structure function is based on the evaluation of the IA diagram (Fig. 1) in which relativistic effects are consistently taken into account, both by keeping the right choice for the components of the four vectors q and p while Bjorken limit is performed [i.e., including the flux factor in Eq. (2.9)], and by a proper identification of the nuclear vertex function $\mathcal{S}_A(p)$, as in Eq. (2.20).

III. SPECTRAL FUNCTIONS, MOMENTUM DISTRIBUTIONS, AND LIGHT CONE MOMENTUM DISTRIBUTIONS USED IN THE CALCULATIONS

The nonrelativistic spectral function is generally defined as[24] (in what follows, the notation $|\mathbf{p}|\equiv k$ will be adopted; moreover, as already pointed out, if the superscripts p and n do not appear explicitly in a given equation, the latter is meant to hold for both protons and neutrons as well as for the summed quantities with proper weights)

$$P(k,E)=(2\pi)^{-3}\sum_f \left|\int d\mathbf{r}\, e^{i\mathbf{k}\cdot\mathbf{r}}G_{f0}(\mathbf{r})\right|^2\delta(E-(E^f_{A-1}-E_A))\ , \tag{3.1}$$

where $G_{f0}(\mathbf{r})$ is the overlap integral between the initial and final wave functions, written in terms of the intrinsic coordinates $\{\mathbf{r},\boldsymbol{\rho}_1\boldsymbol{\rho}_2,\ldots\}$ (spin and isospin variables are omitted)

$$G_{f0}(\mathbf{r})=A^{1/2}\langle\Psi^f_{A-1}(\boldsymbol{\rho}_1,\ldots,\boldsymbol{\rho}_{A-2})|\Psi^0_A(\mathbf{r},\boldsymbol{\rho}_1,\ldots,\boldsymbol{\rho}_{A-2})\rangle\ . \tag{3.2}$$

In Eqs. (3.1) and (3.2), $E=E^f_{A-1}-E_A$ is the nucleon removal energy, E_A is the is ground-state eigenvalue of the A-nucleon Hamiltonian and E^f_{A-1} is the eigenvalue of the state f of the $(A-1)$-nucleon Hamiltonian; writing $E^f_{A-1}=E^{f*}_{A-1}+E_{A-1}$, where $E^{f*}_{A-1}=M^{f*}_{A-1}-M_{A-1}>0$ is the excitation energy of the $(A-1)$-nucleon system, measured from its ground-state energy E_{A-1}, one has $E=E^{f*}_{A-1}+E_{\min}>0$, where $E_{\min}=|E_A|-|E_{A-1}|$. Integrating Eq. (3.1) over the removal energy E, one obtains the momentum distribution $n(k)$

$$n(k)=\int_{E_{\min}}^{\infty} P(k,E)dE \tag{3.3}$$

with normalization condition

$$\int d^3k\, n(k)=1 \ . \tag{3.4}$$

The spectral function represents the joint probability to find in the nucleus A a nucleon with momentum k and removal energy E, or equivalently, the probability to find the $A-1$ system in a state with excitation energy E^{f*}_{A-1} after a nucleon with momentum k has been removed. Therefore for a nucleus with $A \leq 4$, $P(k,E)$ can be represented in the following form.[25]

$$P(k,E)=P_{\rm gr}(k,E)+P_{\rm ex}(k,E) \ , \tag{3.5}$$

where

$$P_{\rm gr}(k,E)=n_{\rm gr}(k)\delta(E-E_{\rm min})$$

("ground-state" spectral function) yields the probability distribution that the final $(A-1)$ system is left in its ground state (corresponding to the excitation energy $E^{f*}_{A-1}=0$ and $E=E_{\rm min}$), whereas $P_{\rm ex}(k,E)$ ("excitation" or "breakup" spectral function) yields the probability distribution that the final $(A-1)$ system is left in any of its excited states (with $E^{f*}_{A-1}>0$, $E=E_{\rm min}+E^{f*}_{A-1}$). Thus, from Eq. (3.3), the following relation between the spectral function and the momentum distribution holds:

$$\begin{aligned} n(k)&=\int_{E_{\rm min}}^{\infty} P(k,E)dE \\ &=n_{\rm gr}(k)+\int_{E_{\rm min}}^{\infty} P_{\rm ex}(k,E)dE \\ &=n_{\rm gr}(k)+n_{\rm ex}(k) \ . \end{aligned} \tag{3.6}$$

The separation (3.5) allows one to single out those effects (nucleon binding and NN correlations effects) that are due to states with $E>E_{\rm min}$ and that manifest themselves only in $P_{\rm ex}$, for in the case of independent particle motion, $E=E_{\rm min}$ and $P_{\rm ex}=0$ [we note in passing that, although the separation (3.5) is valid for any A, in the case of complex nuclei a slightly different representation of the spectral function should be adopted to single out correlations effects (see Ref. 19)]. The integral of the momentum distributions yields the spectroscopic factors

$$S_{\rm gr}=\int d^3k\, n_{\rm gr}(k) \ , \tag{3.7}$$

$$S_{\rm ex}=\int d^3k\, n_{\rm ex}(k) \ , \tag{3.8}$$

which, owing to the normalization for $n(k)$ [Eq. (3.4)], obey the following condition:

$$S_{\rm gr}+S_{\rm ex}=1 \ . \tag{3.9}$$

The mean nucleon kinetic and removal energies in the initial nucleus, and the mean kinetic energy of the $A-1$ system recoiling with momentum $\mathbf{p}_R=-\mathbf{p}$ ($|\mathbf{p}|\equiv k$), are defined as follows:

$$\begin{aligned} \langle T\rangle &= \int d^3k\, dE\, P(k,E)(k^2/2M_N) \\ &=\langle T_{\rm gr}\rangle+\langle T_{\rm ex}\rangle \ , \end{aligned} \tag{3.10}$$

$$\langle E\rangle=\int d^3k\, dE\, P(k,E)E=\langle E_{\rm gr}\rangle+\langle E_{\rm ex}\rangle \ , \tag{3.11}$$

$$\langle T_R\rangle=\int d^3k\, dE\, P(k,E)(k^2/2M_{A-1}) \ . \tag{3.12}$$

As is well known (see, e.g., Refs. 20 and 24), the calculated values of the total energy per nucleon ε_A, of the mean kinetic energy $\langle T\rangle$, and of the mean removal energy $\langle E\rangle$ are linked together by a model-independent relation (energy-weighted sum rule[26]), which reads

$$\langle E\rangle=2|\varepsilon_A|+\langle T\rangle(A-2)/(A-1) \tag{3.13}$$

if the Hamiltonian contains only two-body density independent forces, and

$$\langle E\rangle=2|\varepsilon_A|+\langle T\rangle(A-2)/(A-1)-\langle V_3\rangle \tag{3.14}$$

if a three-body interaction V_3 is also present. Equations (3.13) and (3.14) allow one to obtain the value of $\langle E\rangle$ even if the full spectral function is unknown: indeed, to this end, it is sufficient to know only $n(k)$ (which yields $\langle T\rangle$), ε_A, and $\langle V_3\rangle$. The spectral functions of the three nucleon system has been calculated using three-body wave functions obtained within the variational[22] and the Faddeev[27–29] approaches employing NN realistic interactions, e.g., the Reid soft core (RSC) interaction.[30] For ^{4}He, various variational approaches[31,32] have been adopted. The values of the mean kinetic and removal energies for the three- and four-body systems, are listed in Table I together with the values of the spectroscopic factors. In what follows it will be shown that, as already pointed out in the Introduction, the values of $\langle E\rangle$ and $\langle T\rangle$ are the crucial features of nuclear structure which determine the deviation from one of the ratio $R_A(x,Q^2)$.

In order to obtain the expression for the light cone momentum distribution $f(z)$ within the ansatz (2.20) [the subscript A in $f_A(z)$ whenever possible, will be hereafter omitted], the general procedure is to replace the function $\mathcal{S}_A(p)$ in Eq. (2.8) with the nonrelativistic spectral function properly normalized so as to satisfy the baryon number sum rule [Eq. (2.12)] up to order $\mathbf{p}^2/M_N^2$. By performing the integrations over the directions of $\mathbf{p}$ one gets

$$f(z)=2\pi M_N z C\int_{E_{\rm min}}^{\infty} dE \int_{k_{\rm min}(z,E,M_{A-1})}^{\infty} dk\, kP(k,E) \ , \tag{3.15}$$

where the correct normalization is ensured by the factor C. The lower limit of integration $k_{\rm min}$, which is obtained from the constraint $-1\leq\cos\theta\leq 1$ (θ is the angle between $\mathbf{p}$ and $\mathbf{q}$), reads as follows:

$$k_{\rm min}(z,E,M_{A-1})=\tfrac{1}{2}|(\zeta^2+2M^{f*}_{A-1}\zeta)/(\zeta+M^{f*}_{A-1})| \ , \tag{3.16}$$

where $M^{f*}_{A-1}=E^{f*}_{A-1}+M_{A-1}$ and $\zeta=[M_N(1-z)-E]$. Equation (3.16), which properly takes into account the recoil of the $(A-1)$ system, should always be used in case of few-nucleon systems. Recoil can be disregarded only in the limit $M_{A-1}\gg M_N$; one has in this case $k_{\rm min}=|\zeta|$. Following Eq. (3.5), the light cone momentum distribution can be written in the form

$$f(z)=f_{\rm gr}(z)+f_{\rm ex}(z) \ , \tag{3.17}$$

where

TABLE I. The mean kinetic and removal energies [Eqs. (3.10) and (3.11)], and spectroscopic factors [Eqs. (3.7) and (3.8)] for ^{3}He and ^{4}He. The values for ^{3}He have been obtained using the following quantities for the proton and neutron spectroscopic factors and average energies: $S^p_{gr}=0.65$, $S^p_{ex}=0.35$, $S^n_{gr}=0$, $S^n_{ex}=1$, and $\langle T^p\rangle=15.17$ MeV, $\langle T^n\rangle=21.76$ MeV, $\langle E^p\rangle=11.12$ MeV, $\langle E^n\rangle=18.4$ MeV. The same quantities for ^{3}H can be obtained by exchanging neutrons and protons and vice versa. The total binding energy is $|E_3|=7.3$ MeV and the proton and neutron binding energies are $|\varepsilon_p|=1.77$ MeV and $|\varepsilon_n|=3.76$ MeV, respectively. All these quantities have been obtained in Ref. 22 using a variational spectral function deduced from RSC interaction.[30] The values of the mean kinetic energies for ^{4}He have been obtained from the momentum distribution of Ref. 31 and the values of the mean removal energy using the energy sum rule [Eq. (3.13)]. Other realistic spectral functions and momentum distributions obtained by solving the few-body problem within alternative methods[27–29,32] but using similar *NN* interaction, yield results that differ from the ones presented in this table by less than 10% even when three-body forces are considered.

	$\langle T_{gr}\rangle$ (MeV)	$\langle T_{ex}\rangle$ (MeV)	$\langle T\rangle$ (MeV)	$\langle E_{gr}\rangle$ (MeV)	$\langle E_{ex}\rangle$ (MeV)	$\langle E\rangle$ (MeV)	S_{gr}	S_{ex}
^{3}He	3.2	14.2	17.4	2.4	11.2	13.6	0.64	0.35
^{4}He	8.0	13.1	21.1	15.8	12.4	28.2	0.8	0.2

$$f_{gr}(z)=2\pi M_N z C\int_{k_{min}(z,E_{min},M_{A-1})}^{\infty} dk\, k n_{gr}(k) \tag{3.18}$$

and

$$f_{ex}(z)=2\pi M_n z C \times\int_{E_{min}}^{\infty} dE\int_{k_{min}(z,E,M_{A-1})}^{\infty} dk\, k P_{ex}(k,E)\ . \tag{3.19}$$

For small values of x ($x\le 0.5$) a full calculation of the nuclear structure function [Eq. (2.9)] is not necessary. In fact, by expanding the nucleon structure function in Eq. (2.9) in powers of the variable z around its nonrelativistic value $z=1$, using the baryon number conservation [Eq. (2.12)] and retaining only terms of order $(k/M_N)^2$, one gets

$$F_2^A(x)=\bar F_2^N(x)+x[\partial\bar F_2^N(x/z)/\partial z]_{z=1}\{\langle E\rangle+\langle T_R\rangle-\tfrac{2}{3}\langle T\rangle\}/M_N +\{2x[\partial\bar F_2^N(x/z)/\partial z]_{z=1}+x^2[\partial^2\bar F_2^N(x/z)/\partial z^2]_{z=1}\}\{\tfrac{2}{3}\langle T\rangle\}/M_N\ , \tag{3.20}$$

where the average removal and kinetic energies have to be evaluated directly with the nonrelativistic spectral function and momentum distribution as in Eqs. (3.10)–(3.12). The slope of $R_A(x)$ is governed by the second term in Eq. (3.20), and therefore it crucially depends upon the mean values $\langle E\rangle$, $\langle T_R\rangle$, and $\langle T\rangle$. Moreover, if the coefficients of the power expansion [curly brackets in Eq. (3.20)] are evaluated by disregarding the flux factor in the convolution formula, the term $(\frac{2}{3})\langle T\rangle/M_N=(\frac{1}{3})\langle k^2\rangle/M_N^2$ in the first bracket cancels out, so that the slope of R_A, as we shall see in the following section, is sensibly increased and the EMC effect is strongly enhanced.

IV. RESULTS OF CALCULATIONS

In this section the results of calculations of the ratio $R_A(x,Q^2)$ for $A=2$, 3, and 4, based on the light cone momentum distribution $f_A(z)$, evaluated in terms of momentum distributions and spectral functions resulting from realistic *NN* interactions, will be presented. Calculations have been performed both including and omitting the flux factor and, in the case of ^{4}He, also shell-model results have been obtained. In all numerical calculations, the nucleon structure functions $F_2^{p(n)}$ given in Ref. 33 have been adopted.

A. The two-nucleon system

The nonrelativistic spectral function for the deuteron ($E^*_{A-1}=0$, $E=E_{min}=|E_2|=2.23$ MeV) takes the following obvious form:

$$P(k,E)=n(k)\delta(E-E_{min})\ , \tag{4.1}$$

and therefore is uniquely determined by the nucleon momentum distributions $n(k)$, which can be calculated by exactly solving the two-body problem. Owing to the δ function in Eq. (4.1), the light cone momentum distribution assumes the following simple form:

$$f_D(z)=2\pi M_N z C\int_{k_{min}(z)}^{\infty} dk\, k n(k)\ , \tag{4.2}$$

where $k_{min}(z)$ is obtained from Eq. (3.16) placing $M^{f*}_{A-1}=M_N$ and $E=E_{min}$. The quantity that must be compared to the experimental data is in this case

$$R_D(x,Q^2)=\frac{F_2^D(x,Q^2)}{\bar F_2^N(x,Q^2)}=\frac{\int_{x\le z} dz\, f_D(z)[F_2^p(x/z,Q^2)+F_2^n(x/z,Q^2)]/2}{[F_2^p(x,Q^2)+F_2^n(x,Q^2)]/2}\ . \tag{4.3}$$

The ratio $R_D(x,Q^2)$ is shown in Fig. 2 where the results obtained including and omitting the flux factor are presented in order to show the "damping" effect caused by the latter. It should be noticed that the depletion of $R_D(x,Q^2)$ in the region $0.2 \leq x \leq 0.6$ is not due to nucleon binding, which in the deuteron is very small, but to the relatively high value of the recoil kinetic energy which affects both the power expansion (3.20) (through the term $\langle T_R \rangle = \langle T \rangle = 11.5$ MeV), as well as the exact calculation (by increasing the value of $k_{\min}$ in $f_D(z)$ [Eq. (4.2)]). Although the experimental uncertainties in the determination of $R_D(x,Q^2)$ (essentially due to the poor information on the neutron deep inelastic structure function) are very large, it is nonetheless important to use the correct theoretical deuteron structure function F_2^D in the evaluation of the ratio R_A for heavier nuclei [Eqs. (2.15)–(2.18)]. In fact, both the 2–4% difference between $F_2^D(x)$ and $\bar{F}_2^N(x)$ in the region $0.2 \leq x \leq 0.65$, and the tail of $F_2^D(x)$ at $x > 0.65$ due to the high momentum behavior of $f_D(z)$, do affect the ratio R_A for heavier nuclei, for which the maximum depletion of the experimental data occurs at $x \approx 0.65$ and is of the order of 15–20%.

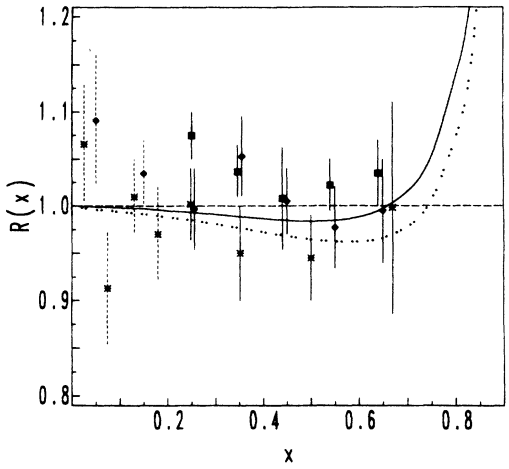

FIG. 2. The ratio $R_D(x)=F_2^D(x)/\bar{F}_2^N(x) \equiv R(x)$ in deuteron [Eq. (4.3)]. In the full curve the flux factor z is considered in the calculation of the light cone momentum distribution [Eq. (4.2)], whereas in the dotted line such factor is disregarded, i.e., it is set equal to one. The deuteron momentum distribution is obtained from the Reid Soft Core (RSC) interaction.[30] In this figure and in the following ones, the free nucleon structure function taken from Ref. 33 has been used. Experimental data from Ref. 34.

B. The three-nucleon systems

Since we are now concerned with nonisoscalar nuclei, the proton and neutron spectral functions and momentum distributions have to be explicitly distinguished; one therefore has

$$P(k,E)=(Z/A)P^p(k,E)+(N/A)P^n(k,E) , \tag{4.4}$$

$$n(k)=(Z/A)n^p(k)+(N/A)n^n(k) . \tag{4.5}$$

Introducing the isospin T of the spectator pair, the following decomposition for ^{3}He is obtained

$$P^p(k,E)=(\tfrac{3}{4})P^p_{T=0}(k,E)+(\tfrac{1}{4})P^p_{T=1}(k,E) , \tag{4.6}$$

$$P^n(k,E)=P^n_{T=1}(k,E) , \tag{4.7}$$

where in $P^p_{T=0}(k,E)$, $P^p_{T=1}(k,E)$, and $P^n_{T=1}(k,E)$, the spectator pair is a deuteron, a proton-neutron pair and a proton-proton pair, respectively, each P_T being normalized to one. If the Coulomb interaction between nucleons is disregarded, one has

$$P^p(^3\mathrm{He})=P^n(^3\mathrm{H}) , \tag{4.8}$$

$$P^n(^3\mathrm{He})=P^p(^3\mathrm{H}) . \tag{4.9}$$

The total light cone momentum distribution can thus be written as

$$f(z)=(Z/A)f^p(z)+(N/A)f^n(z) , \tag{4.10}$$

where, following Eq. (3.15), the functions $f^{p(n)}(z)$ are given by

$$f^{p(n)}(z)=2\pi MzC \int_{E_{\min}}^{\infty} dE \times \int_{k_{\min}(z,E,M_{A-1})}^{\infty} dk\, kP^{p(n)}(k,E) . \tag{4.11}$$

In Eq. (4.11) $E_{\min}$ is equal to 5.5 MeV in ^{3}He and 6.3 MeV in ^{3}H and M_{A-1} is either the deuteron mass or the mass of two nucleons. The ratio $R_3(x)$ for ^{3}He is thus given by

$$R_3(x,Q^2)=\frac{\int_{x\leq z} dz\,[(\frac{2}{3})f^p(z)F_2^p(x/z,Q^2)+(\frac{1}{3})f^n(z)F_2^n(x/z,Q^2)]}{\int_{x\leq z} dz\, f_D(z)[F_2^p(x/z,Q^2)+F_2^n(x/z,Q^2)]/2} \frac{[F_2^p(x)+F_2^n(x)]/2}{[2F_2^p(x)+F_2^n(x)]/3} , \tag{4.12}$$

whereas the same quantity for ^{3}H is obtained by exchanging protons with neutrons, and viceversa. In the case of ^{3}He, the possible final states are $d+p$, $(pn)+p$, $(pp)+n$. This means that, whereas the neutron spectral function $P^n(k,E)$ describes only excited configurations, the proton spectral function $P^p(k,E)$ contains both ground and excited parts, so that in Eq. (4.12), according to Eq. (3.5), $f^p(z)$ is given by

$$f^p(z)=f^p_{\mathrm{gr}}(z)+f^p_{\mathrm{ex}}(z) . \tag{4.13}$$

Both the effects of separating in $P(k,E)$ the contribution of the two-body system in its ground and excited states, respectively, and of considering the different distributions of protons and neutrons, were analyzed in our calculation of the ratio R_3. Moreover, the calculations were performed both including and omitting the flux factor z in

the convolution formula for both the three-body system and the deuteron structure functions. The results are shown in Figs. 3 and 4.

The ratio $R_3(x)$ for ^{3}He, evaluated both including and omitting the factor z, as well as by disregarding the EMC effect in the deuteron, is presented in Fig. 3, whereas in Fig. 4 the ratios R_3 for ^{3}He and ^{3}H are compared. It can be seen from Fig. 3, that the flux factor has a large impact on the quantitative evaluation of the ratio R_3, since it yields a relativistic correction [corresponding to the quantity $(\frac{2}{3})\langle T\rangle/M_N$ in Eq. (3.20)], which reduces the effect of nucleon dynamics in determining the depletion expected in the region $0.2 \leq x \leq 0.65$. In previous calculations of the EMC effect in the three-body systems, also based upon exact realistic three-body spectral functions,[23,35] the flux factor was not included. Moreover, the theoretical predictions were compared with the experimental data for ^{4}He, which turned out to strongly disagree with the theoretical results in the region $x \leq 0.6$. Since the dynamical features in three- and four-nucleon systems, in particular the values of $\langle T\rangle$ and $\langle E\rangle$, which affect the slope of R_3, are different (cf. Table I), the experimental data for the two systems are not expected, in principle, to show a similar behavior. From the general A dependence observed in Ref. 3, one may argue that the data for ^{3}He or ^{3}H should be located closer to unity than the experimental data for ^{4}He. The shaded area in Fig. 3 represents an expectation for the EMC data in the three-body system, obtained by "rescaling" the experimental points for ^{4}He following an ansatz given in Ref. 13 and obtained from a comparison of mean nuclear densities in

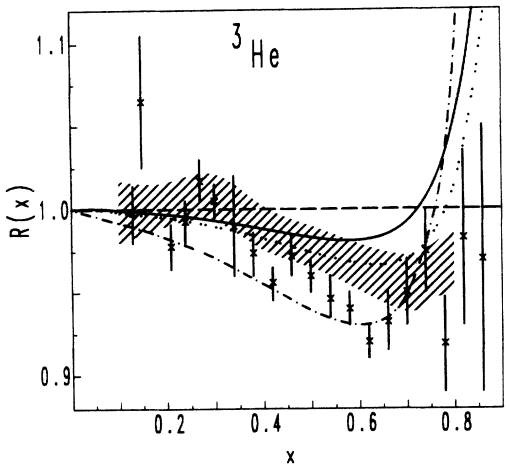

FIG. 3. The ratio $R_3(x)\equiv R(x)$ in ^{3}He [Eq. (4.12)]. All curves were calculated using the exact spectral function of Ref. 22; in the solid curve the flux factor was taken into account while in the dotted curve it was omitted. The dot-dashed curve was obtained by disregarding the EMC effect in deuteron, i.e., by placing in the denominator of Eq. (4.12), the average nucleon structure function $\bar{F}_2^N(x)=\{F_2^p(x)+F_2^n(x)\}/2$, instead of Eq. (2.16). The experimental data are from Ref. 3 and refer to the ^{4}He nucleus; the shaded area represents a prediction for the possible location of the experimental data for the three-body system, obtained by taking the average of the rescaled ^{4}He data from Ref. 3, following the ansatz given in Ref. 13.

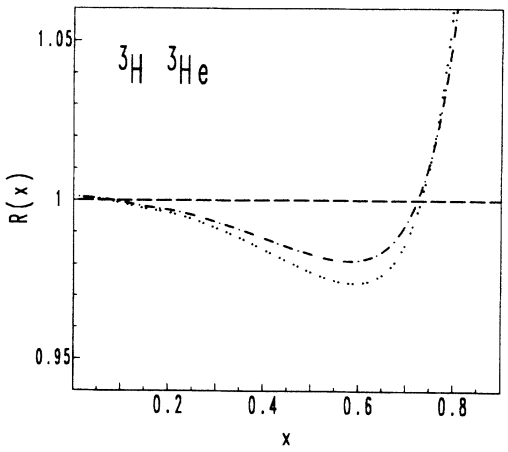

FIG. 4. The ratio $R_3(x)\equiv R(x)$ in ^{3}He (dot-dashed curve) and ^{3}H (dashed curve). The difference between the two curves is due to the different proton and neutron spectral functions in the two nuclei.

the two systems. It can be seen that the full curve sharply disagrees with the ^{4}He data, whereas it is in much better agreement with the rescaled data. Experimental data for ^{3}He are therefore urgently called for.

As far as Fig. 4 is concerned, the difference between the two curves is due both to the differences between the proton and neutron structure functions F_2^p and F_2^n, as well as between the proton and neutron spectral functions $P^p(k,E)$ and $P^n(k,E)$. These differences, however, do not strongly affect the ratio R_3. Such a result can be explained by observing that (i) in the region $x \leq 0.6$ the EMC effect mostly depends upon the mean values of the removal and kinetic energies, which are not very different for protons and neutrons; (ii) the difference between the free proton and neutron structure functions is reduced by the isoscalarity correction factor [Eq. (2.17)]. Moreover, for $x \to 1$ the ratio R_3 essentially depends upon the integral of the high momentum tail of the momentum distributions and since there is again no sensible difference between ^{3}He and ^{3}H integrated quantities [cf. the average values of the kinetic energy, which crucially depend upon the high momentum behavior in $n(k)$], the results are quite similar.

Thus, our main conclusion concerning the behavior of the ratio R_3 for the three-body system in the $x < 1$ region, is that the EMC effect does not depend upon the details of the spectral function, being only sensitive to the mean values of the kinetic and removal energies. Therefore, one expects that the following approximation for the proton or neutron break-up spectral functions, viz.,

$$P_{\rm ex}(k,E)=n_{\rm ex}(k)\delta(E-\bar{E}_{\rm ex}) \tag{4.14}$$

could be adopted for the calculation of the EMC effect. In Eq. (4.14) the quantity $\bar{E}_{\rm ex}$ is related (see further on) to the average value of the removal energy of the breakup configurations for the $A-1$ system. The ansatz (4.14) has the advantage that $n_{\rm ex}(k)$ for $A>3$ is known from explicit calculations, whereas $\bar{E}_{\rm ex}$ can easily be obtained

from the general definition of the mean removal energy. In fact, from Eqs. (3.11) and (4.14) one gets for the average removal energy (e.g., for a proton in ^{3}He or for a nucleon in an isoscalar nucleus)

$$\langle E\rangle = E_{\min}\int d^3\mathbf{k}\, n_{\rm gr}(k) + \bar{E}_{\rm ex}\int d^3\mathbf{k}\, n_{\rm ex}(k) = \langle E_{\rm gr}\rangle + \langle E_{\rm ex}\rangle \ , \tag{4.15}$$

where $\langle E_{\rm gr}\rangle = E_{\min} S_{\rm gr}$ and $\langle E_{\rm ex}\rangle = \bar{E}_{\rm ex} S_{\rm ex}$, from which $\bar{E}_{\rm ex}$ can be obtained as follows:

$$\bar{E}_{\rm ex} = \langle E_{\rm ex}\rangle / S_{\rm ex} \ . \tag{4.16}$$

Using the calculated values for $\langle E_{\rm ex}\rangle$ and $S_{\rm ex}$, given in Table I, the following values of $\bar{E}_{\rm ex}$ in ^{3}He are obtained: $\bar{E}^p_{\rm ex} = 21.6$ MeV and $\bar{E}^n_{\rm ex} = 18.4$ MeV. Placing Eq. (4.14) in Eq. (3.19) one finally gets

$$f_{\rm ex}(z) = 2\pi M_N z C \int_{k_{\min}(z,\bar{E}_{\rm ex},M_{A-1})}^{\infty} dk\, k n_{\rm ex}(k) \ . \tag{4.17}$$

The validity of the ansatz (4.17) has been checked by comparing the ratio $R_3(x)$ [Eq. (4.12)] calculated exactly, and within the approximation (4.17). The results are presented in Fig. 5 from which it can be seen that there is no relevant difference between the two cases. The application of the ansatz (4.17) to the evaluation of the EMC effect in ^{4}He and complex nuclei,[19] for which $n_{\rm ex}$ has been calculated but the exact nonrelativistic spectral function is not yet available, appears, therefore, fully justified.

C. The four-nucleon system

The ratio R_4 has been evaluated by separating the ground and excited parts of the spectral function using the approximation for $P_{\rm ex}(k,E)$ given by Eq. (4.14). The nucleon momentum distribution in ^{4}He has been calculated by different authors using various types of NN interactions, including also three-body forces.[31,32] As in the case of three body system (see Ref. 22), the momentum distribution for $k > 1.5$–2 fm^{-1} is entirely exhausted by $n_{\rm ex}$, i.e., by ground-state configurations characterized by high virtual excitations of the $A-1$ spectator system, which means that the removal energy associated to $P_{\rm ex}(k,E)$ corresponds to breakup channels of the $A-1$ nucleus with values of E much higher than typical shell-model values. Since ^{4}He is an isoscalar nucleus, proton and neutron quantities coincide and the ratio R_4 is given by [cf. Eq. (2.18)]

$$R_4(x,Q^2) = \frac{\int_{x\le z} f_4(z)\bar{F}_2^N(x/z,Q^2)dz}{\int_{x\le z} f_D(z)\bar{F}_2^N(x/z,Q^2)dz} \ , \tag{4.18}$$

where

$$f_4(z) = 2\pi M_N z C \left[\int_{k_{\min}(z,E_{\min},M_{A-1})}^{\infty} dk\, k n_{\rm gr}(k) + \int_{k_{\min}(z,\bar{E}_{\rm ex},M_{A-1})}^{\infty} dk\, k n_{\rm ex}(k)\right] \tag{4.19}$$

with the value of $\bar{E}_{\rm ex}$ obtained from Eq. (4.16), using for $S_{\rm ex}$ and $\langle E_{\rm ex}\rangle$ the values listed in Table I. The contributions of the ground and the excited parts of the spectral function to the ratio R_4, are shown in Fig. 6. It can be seen that around $x \approx 1$, the role of correlations (which generate $P_{\rm ex}$) becomes very important. The light cone momentum distribution $f_4(z)$ multiplied by the nucleon structure function $\bar{F}_2^N(x/z)$ is shown in Fig. 7 for different values of x; the role played by the average removal energy and by the high momentum components is clearly demonstrated. In fact, for small values of x, the integral over z of the function $[f_4(z)F_2^N(x/z)]$, is practically governed by the value assumed at the peak ($z_{\rm peak} \approx 1 - \langle E\rangle / M_N$), since the tails of the function lie at

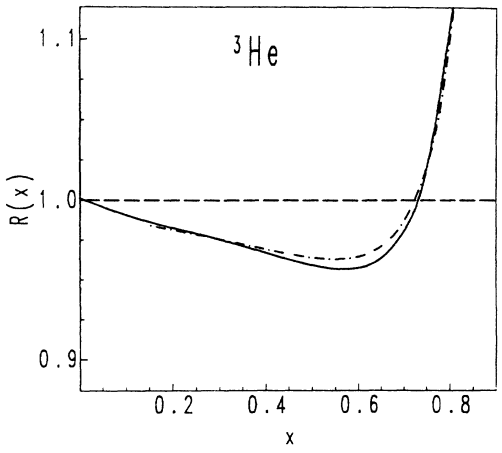

FIG. 5. The ratio $R_3(x) \equiv R(x)$ in ^{3}He calculated using the exact spectral function of Ref. 22 (dot-dashed curve) and the approximated form corresponding to Eq. (4.14) (solid curve). For the sake of simplicity, the flux factor and the recoil energy were not included in the calculation.

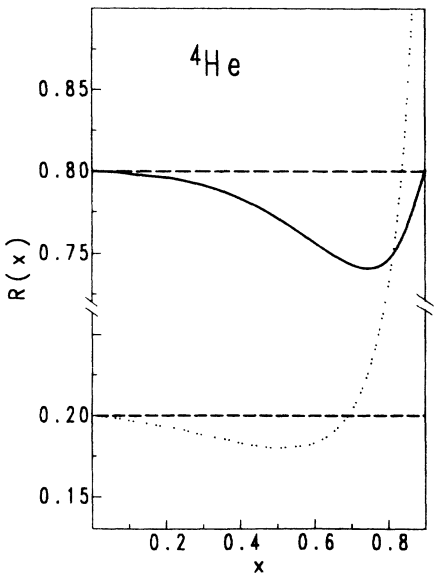

FIG. 6. The effect of the separation of the ground and excited parts of the spectral function on the ratio $R_4(x) \equiv R(x)$ for ^{4}He [Eq. (4.18)]. The solid curve represents the contribution of the ground part and the dotted curve the contribution of the excited part [see Eqs. (3.5), (3.6), and (4.19)]. The total ratio $R_4(x)$ is given by the sum of the two contributions.

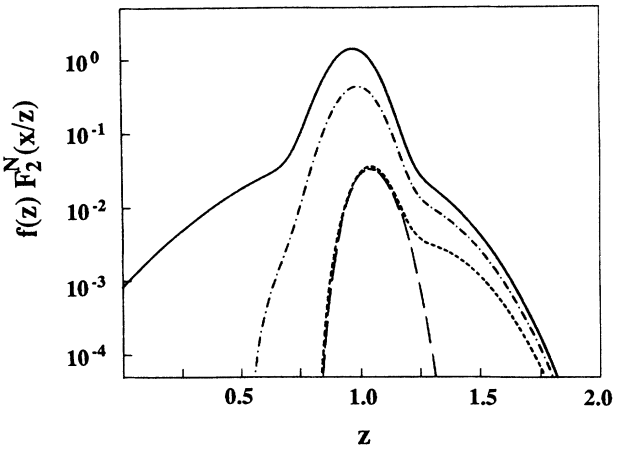

FIG. 7. The function $[f(z)\bar{F}_2^N(x/z)]$ in ^{4}He for different values of Bjorken's variable x. It can be seen that for small values of x the relevant quantity in the convolution formula is the value assumed by this function at the peak, which mainly depends upon the value of $\langle E \rangle$; at high values of x, the role of the tail generated by correlations becomes increasingly important. Solid curve: $x=0$; dot-dashed curve: $x=0.5$; short-dashed curve: $x=0.8$. For $x=0.8$ the quantity $[f_{\rm gr}(z)\bar{F}_2^N(x/z)]=0.8[f_{\rm SM}(z)\bar{F}_2^N(x/z)]$ is also shown (long-dashed curve).

least 2 orders of magnitude below the maximum; on the other hand, the tail generated by correlations, strongly affects the behavior of $F_2^A(x)$, at $x \approx 1$.

In Refs. 10 and 12, a shell-model (SM) spectral function has been adopted, viz.

$$P^{\rm SM}(k,E)=1/(4\pi A)\sum_\alpha A_\alpha n_\alpha^{\rm SM}(k)\delta(E-|\varepsilon_\alpha|)\ , \quad (4.20)$$

where A_α is the number of nucleons in the orbital $\alpha(\sum_\alpha A_\alpha = A)$, the sum over α runs over the states below the Fermi level, and $n_\alpha^{\rm SM}(k)$ is the SM momentum distribution of the state α with single-particle energy ε_α. For ^{4}He, $A_\alpha=4$, $\alpha=1s$, and the light cone momentum distribution assumes the following form:

$$f(z)=2\pi M_N z\{1/(4\pi)\int_{k_{\rm min}(z,|\varepsilon_{1s}|,M_{A-1})}^{\infty} n_{1s}^{\rm SM}(k)k\,dk\}\ , \quad (4.21)$$

where $|\varepsilon_{1s}|=19.8$ MeV and $k_{\rm min}$ is calculated from Eq. (3.16).

The values of the mean removal and kinetic energies used in our approach (denoted SRC) are presented in Table II, where they are compared with the shell-model values. The ratio R_4 obtained with the SM and SRC spectral functions, is shown in Fig. 8. It can be seen that if the flux factor is taken into account, the experimental data cannot be interpreted within a SM picture, due to the low values of $\langle T \rangle$ and $\langle E \rangle$; on the contrary, when correlations are included, the increase they produce on $\langle T \rangle$ and $\langle E \rangle$ strongly enhances the EMC effect.

The agreement between theoretical calculations and experimental data in the range $0.2<x<0.7$ is highly satisfactory, particularly in the light of the fact that no free parameters are present in our approach. Nonetheless, an appreciable disagreement between theory and experiments can be observed in the region $0.7 \le x \le 1$, which is a feature also present in complex nuclei.[19] In the region $x \approx 1$, the experimental data are very sensitive to correlations and therefore to the detailed energy dependence of the spectral function. Calculations with improved spectral functions are therefore highly necessary; these are in progress and will be presented elsewhere.

In order to illustrate the relevant role played by the flux factor, as well as by the deuteron structure function appearing in the denominator of the ratio $R_A(x)$, we have analyzed the behavior of the first terms in the series expansions [Eq. (3.20)] for $F_2^A(x)$ and $F_2^D(x)$, i.e.,

$$F_2^{A(D)}(x)=1+(c_{A(D)}/M_N)x[\partial\bar{F}_2^N(x/z)/\partial z]_{z=1}\ , \quad (4.22)$$

where

$$c_{A(D)}=\langle E \rangle_{A(D)}+\langle T_R \rangle_{A(D)} \quad (4.23)$$

if the flux factor is disregarded, and

$$c_{A(D)}=\langle E \rangle_{A(D)}+\langle T_R \rangle_{A(D)}-\tfrac{2}{3}\langle T \rangle_{A(D)}\equiv c_{A(D)}^{(z)} \quad (4.24)$$

when the flux factor is taken into account. It can easily be shown that the difference $\Delta=c_A-c_D$ ($\Delta^{(z)}=c_A^{(z)}-c_D^{(z)}$) determines the slope of $R_A(x)$ for $A>2$ in the region $x \le 0.4$, where the effect of Fermi motion is still very small. The values of the coefficients $c_{A(D)}$ and $c_{A(D)}^{(z)}$, and of the quantities Δ and $\Delta^{(z)}$ are listed in Table III. It can be noticed that (i) the quantities Δ and $\Delta^{(z)}$ increase with A (and so does, consequently, the slope of R_A); (ii) because of the presence of the flux factor, the values of $\Delta^{(z)}$

TABLE II. Spectroscopic factors [Eqs. (3.7) and (3.8)] and nucleon mean kinetic and removal energies in ^{4}He [Eqs. (3.10) and (3.11)]; the last column shows the quantity $\bar{E}_{\rm ex}$ [Eq. (4.16)] associated to breakup configurations. All quantities denoted SRC correspond to the four-body calculation of Ref. 31 performed with Reid $V6$ interaction. The corresponding quantities resulting from the approach of Ref. 32, where Urbana $V14$ interaction (Ref. 36) plus three-body forces were employed, differ by the ones listed in the table by at most 10%. The quantities denoted SM correspond to the shell model results with $\langle E \rangle=|\varepsilon_{1s}|$ and $\langle T \rangle$ calculated using harmonic oscillator wave functions which reproduce the rms radius.

	$S_{\rm gr}$	$S_{\rm ex}$	$\langle T_{\rm gr} \rangle$ (MeV)	$\langle T_{\rm ex} \rangle$ (MeV)	$\langle T \rangle$ (MeV)	$\langle E_{\rm gr} \rangle$ ((MeV)	$\langle E_{\rm ex} \rangle$ (MeV)	$\langle E \rangle$ (MeV)	$\bar{E}_{\rm ex}$ (MeV)
SRC	0.8	0.2	8.0	13.1	21.1	15.8	12.4	28.2	62.0
SM	1	0	17.1	0	17.1	19.8	0	19.8	0

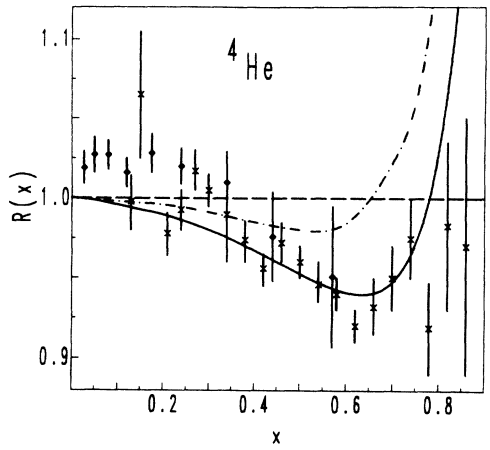

FIG. 8. Comparison between theoretical calculations and experimental data for ^{4}He. Both curves represent the ratio $R_4(x)=F_2^A(x)/F_2^D(x)\equiv R(x)$ [Eq. (4.18)]. The solid curve corresponds to the correlated light cone momentum distribution [Eq. (4.19)], whereas the dot-dashed curve was obtained within a Shell-model approach [Eqs. (4.20) and (4.21)]. Experimental data are from Ref. 3 (crosses) and Ref. 5 (diamonds). Both curves include the flux factor. If the latter is disregarded, the values of the ratio $R(x)$ at the minima are: $R(0.65)=0.92$, for our correlated approach, and $R(0.60)=0.96$, for the SM case.

are lower than the values of Δ; (iii) if nuclear effects in deuteron are disregarded, i.e.,

$$F_2^{(D)}(x)=[F_2^n(x)+F_2^p(x)]/2 ,$$

one has $\Delta\to c_A$ and $\Delta^{(z)}\to c_A^{(z)}$, and thus the slope of $R_A(x)$ is enhanced (cf., e.g., the dot-dashed line in Fig. 3).

Although our description of the EMC effect in terms of strongly correlated nucleons appears to be a satisfactory one, it should be remembered that a feature of our calculation, which is common to all models relying on the IA with nucleonic degrees of freedom only, is that the trend of EMC data can be reproduced only in spite of a violation of the momentum sum rule, which can be written in terms of the light cone momentum distribution, in the following form:

$$\int dz\, f_A(z)z=\eta<1 , \tag{4.25}$$

where η is the total light cone momentum carried by nucleons and $(1-\eta)$ is the missing fraction of the total nuclear light cone momentum. The sum rule is restored by assuming that non-nucleonic components carry the fraction $(1-\eta)$ of the missing momentum.[7,10] In this sense the EMC effect clearly demonstrates the presence of non-nucleonic components in nuclei. However, as one may argue from Eq. (4.25), before any quantitative prediction on the contribution of non-nucleonic degrees of freedom could be done, the quantity η should be evaluated within realistic approaches to the nuclear structure, as suggested by the results of present calculations. The values of the quantity η obtained in our approach, are presented in Table IV, where, in the case of ^{4}He, also the SM predictions are given. It can be seen that both the flux factor and *NN* correlations affect the momentum sum rule.

V. Q^2 RESCALING

Several models for the interpretation of the EMC effect have been proposed, based on the modification of nucleon properties inside the nucleus. One of the most popular ones is the Q^2-rescaling mechanism of Ref. 8, where it was observed that the trend of EMC data can be explained, for $0.2\le x\le 0.7$, by setting

$$F_2^A(x,Q^2)\cong\bar{F}_2^N(x,\xi(Q^2)Q^2) \tag{5.1}$$

with the parameter ξ larger than unity. The Q^2 dependence of ξ in Eq. (5.1) is determined so as to satisfy the QCD evolution equations on both sides of the equation

TABLE III. Mean removal $\langle E\rangle$ and recoil $\langle T_R\rangle$ energies in ^{2}H, ^{3}He, and ^{4}He and coefficients $c_{A(D)}$ and $c_{A(D)}^{(z)}$ [Eqs. (4.23) and (4.24)] of the first terms in the series expansion [Eq. (4.22)], including $[c_{A(D)}^{(z)}]$ and disregarding $(c_{A(D)})$ the flux factor. The quantities $\Delta=c_A-c_D$ and $\Delta^{(z)}=c_A^{(z)}-c_D^{(z)}$ govern the slope of $R_A(x)$ in the region of small x ($x\le 0.4$). For ^{2}H and ^{3}He the results of the present paper are compared with the ones of Ref. 23 where a realistic three-body spectral function obtained[29] from Faddeev equations has been employed. For ^{4}He the correlated many-body approach of this paper is compared with single particle shell-model results of Ref. 10.

	$\langle E\rangle$ (MeV)	$\langle T_R\rangle$ (MeV)	$c_{A(D)}$ (MeV)	$c_{A(D)}^{(z)}$ (MeV)	Δ (MeV)	Δ_z (MeV)
^{2}H						
a	2.23	11.50	13.73	6.06		
b	2.23	11.05	13.28	5.91		
^{3}He						
a	13.6	8.71	22.31	10.71	8.58	4.65
b	11.35	6.32	17.67	5.1	4.39	−0.81
^{4}He						
a	28.2	7.1	35.3	21.2	21.57	15.14
c	19.8	5.7	25.5	14.17	11.77	8.11

[a]This paper.
[b]Reference 23.
[c]Reference 10.

TABLE IV. The value of the momentum sum rule [Eq. (4.25)] for ^{2}H, ^{3}He, and ^{4}He obtained including and disregarding the flux factor in the definition of $f_A(z)$ [Eq. (2.11)]. For ^{4}He the results obtained within the present approach are compared with the ones obtained using a shell-model spectral function [Eq. (4.20)].

	^{2}H	^{3}He	^{4}He
η (including the flux factor)	0.993	0.989	0.977[a] 0.985[b]
η (omitting the flux factor)	0.985	0.976	0.962[a] 0.973[b]

[a]Present calculations.
[b]Shell-model calculations of Ref. 10.

and the additional hypothesis is made that the quark confinement radius for a bound nucleon (λ_A) is larger than that for a free nucleon (λ_N) (dynamical rescaling) according to the ansatz

$$\lambda_A^2/\lambda_N^2=\mu_N^2/\mu_A^2=\xi(\mu_A^2)\ , \tag{5.2}$$

where μ_A and μ_N are the lower momentum cutoffs for the bound and free nucleon, respectively. The following expression is then obtained for the rescaling factor:

$$\xi(Q^2)=\{(\lambda_A/\lambda_N)^2\}^{\ln(Q^2/\Lambda^2)/\ln(\mu_A^2/\Lambda^2)}\ , \tag{5.3}$$

where Λ is the universal QCD scale parameter, whose experimental value is $\Lambda=250\pm100$ MeV.[8] Since the initial hypothesis is that $\lambda_A>\lambda_N$ and, moreover, $Q^2>\Lambda^2$ and $\mu_A^2>\Lambda^2$ (in Ref. 8 μ_A ranges from 0.50 GeV^2 in iron to 0.66 GeV^2 in deuteron), one has that $\xi(Q^2)$ is larger than one for any Q^2 value corresponding to the DIS kinematical region.

Several models could be advocated to justify the increase of the confinement size in bound nucleons, like, e.g., the hypothesis of overlapping between nucleon bags leading to the formation of multiquark bags,[8] the idea of swelling of the individual nucleons imbedded in the nuclear medium (see, e.g., Ref 37), the model proposed in Ref. 12, in which the parameter ξ increases its value due to the nucleon off shellness. Rescaling effects have been recently investigated within the convolution formula approach,[12,18,19] i.e., by replacing Q^2 with the quantity $\xi(Q^2)Q^2$ in $\bar{F}_2^N(x/z,Q^2)$ which appear in Eq. (2.18). In this paper the same approach has been followed. Namely, we have replaced Q^2 by $\xi(Q^2)Q^2$ in the nucleon structure function appearing in Eqs. (4.12) and (4.18) and have varied the quantity λ_A/λ_N so as to fit the experimental data. The results are shown in Fig. 9 and the best fit values for λ_A/λ_N and $\xi(Q^2)$ are listed in Table V, together with the corresponding values obtained in Ref. 8. It can be noticed that if Q^2 rescaling is introduced within the convolution formula in which high nucleon momenta and removal energy components which largely affect the slope of $R_A(x,Q^2)$ are present, the EMC effect might be strongly overestimated, i.e., the theoretical $R_A(x,Q^2)$ is located much lower than the experimental data. In order to fit the latter, only a small increase (of the order of three percent) of the quark confinement radius of a bound nucleon seems to be necessary, in agreement with the results of y-scaling analysis[38,39] of inclusive quasielastic data.[40] We believe, therefore, that our results point to the necessity of a realistic treatment of nucleon dynamics, before any conclusive information on bound nucleon properties could be extracted from DIS cross sections.

TABLE V. The ratio λ_A/λ_N [Eq. (5.2)] of the confinement radii for bound (λ_A) and free (λ_N) nucleons, respectively, and the rescaling parameter ξ [Eq. (5.3)] at $Q^2=20$ GeV^2 for ^{3}He and ^{4}He. The results obtained in Ref. 8 using Eq. (5.1) are compared with the values obtianed in our approach using Eq. (5.3) in the convolution formula (2.9).

	λ_A/λ_N	ξ ($Q^2=20$ (GeV/c)^2)
	^{3}He	
a	1.040	1.20
b	1.025	1.12
	^{4}He	
a	1.079	1.43
b	1.025	1.15

[a]Close *et al.* (Ref. 8).
[b]This paper.

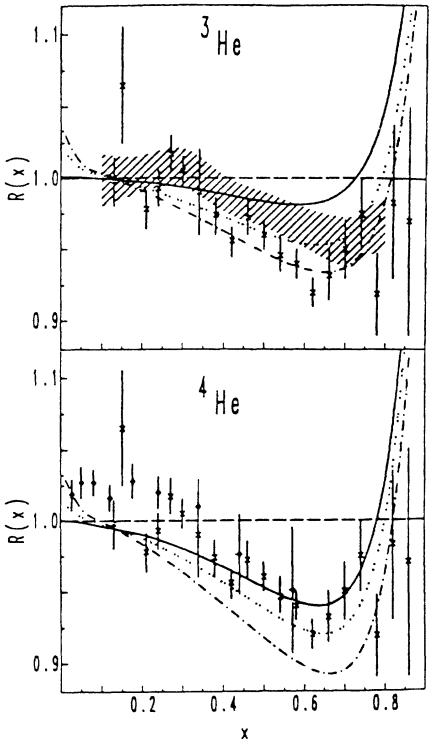

FIG. 9. The effect of Q^2 rescaling in ^{3}He and ^{4}He. The solid curves were obtained within the present correlated approach (cf. Figs. 3 and 8). The dotted curves, which represent the best fits to the experimental data, were obtained by including also the effect of Q^2 rescaling in the convolution formula with a 2.5% increase of the quark confinement radius in both nuclei (cf. the values of λ_A/λ_N in Table V); in the dot-dashed curves the confinement radius was increased by 4% in ^{3}He and by 7.9% in ^{4}He (see Table V).

VI. THE STRUCTURE FUNCTION OF THE THREE-NUCLEON SYSTEM FOR $x \geq 1$

The formalism adopted in the previous sections, can be easily extended to the calculation of the ratio R_A in the region $x > 1$. In this case the nucleonic contribution to the DIS nuclear structure function is mainly determined by the integral over the high momentum and high removal energy components of the spectral function, which govern the behavior of the light cone momentum distribution $f(z)$ for $z > 1$ (see Fig. 7). Since the nucleon Fermi motion is expected to dominate the large x behavior of the nuclear structure function, several authors[6,41] have calculated F_2^A for complex nuclei, taking only into account the Fermi motion and disregarding the nucleon removal energy. The main result of Refs. 6 and 41, which essentially employed phenomenological nuclear matter momentum distributions, is that a nonvanishing value of the nuclear structure function for values of x larger than $x \approx 1 + k_F/M_N$ (k_F being the Fermi momentum), requires a tail of $n(k)$ for $k > k_F$, which can only be provided by NN correlations. Disregarding nucleon removal energy at $x > 1$ does not seem to be, in principle, a fully justified assumption. In fact, as clearly illustrated in Ref. 22, the nucleon high momentum components are always linked to nucleon high removal energies, in that the larger the value of k in Eq. (3.3), the larger the value of the upper limit of integration which is necessary to obtain the saturation of $n(k)$; for example, the results of Ref. 22 show that the nucleon momentum distribution in ^{3}He is already saturated at $k \approx 1$ fm^{-1} by integrating Eq. (3.3) from $E_{\min} = 5.5$ MeV to $E_{\max} = 10$ MeV, whereas, in order to obtain saturation at $k \approx 3$ fm^{-1}, the upper limit of integration has to be extended up to at least 200 MeV (see Fig. 3 of Ref. 22). Thus, the integration of Eq. (3.19) over the high value of k, which governs the behavior of $f(z)$ for $z > 1$, and therefore, the behavior of F_2^A for $x > 1$, is always associated to high values of the removal energy E; the latter is therefore expected to play an important role even at $x > 1$. In order to investigate such a problem, the three-body structure function $F_2^3(x,Q^2)$ and the ratio $R_3(x,Q^2)$ have been calculated within our approaches in which the link between high momentum and high removal energy components is correctly taken into account in the exact spectral function. The results of calculations are presented in Figs. 10 and 11, where the predictions of the approach based on the exact spectral function are compared with the results obtained using only the momentum distributions and two approximate spectral functions, namely the one given by Eq. (4.14), and the following one

$$P_{\rm ex}(k,E) = n_{\rm ex}(k)\delta(E - k^2/4M_N) \tag{6.1}$$

which approximately takes into account two nucleon correlations (see Refs. 13 and 42). It can be seen from the results presented in Fig. 10, that at $x > 1$ binding effects are really important and decrease the structure function

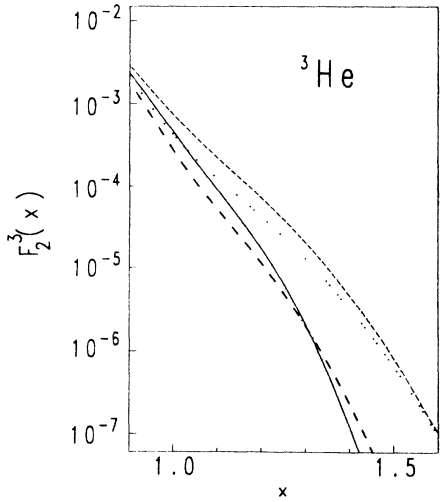

FIG. 10. The nuclear structure function F_2^3 of ^{3}He for $x \geq 0.9$. Different curves correspond to different types of spectral functions. Dotted curve: approximation given by Eq. (4.14); solid curve; spectral function given by Eq. (6.1) which takes into account only two-nucleon correlations [Refs. 13(b) and 42]; dot-dashed curve: exact spectral function of Ref. 22. The dashed curve has been obtained by disregarding binding effects and taking into account only the Fermi motion.

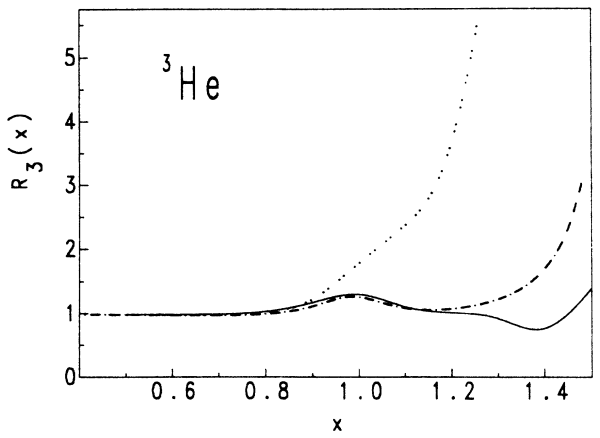

FIG. 11. The ratio $R_A(x)$ for ^{3}He for $x \geq 0.4$. Different curves correspond to different types of spectral functions. Dotted curve: approximation given by Eq. (4.14); solid curve: spectral function given by Eq. (6.1) which takes into account only two-nucleon correlations;[13b,42] dot-dashed curve: exact spectral function of Ref. 22.

with respect to the case in which nucleon binding is disregarded. Our results agree with the ones of Ref. 43, where the structure function F_2^A was calculated at $x \geq 1$ using a model spectral function for nuclear matter (NM) including 2p-2h excitations. The dependence of DIS nuclear structure functions upon the removal energy is better visualized by plotting the ratio R_A, rather than the structure functions themselves, since, by this way, various approximations for the spectral functions produce qualitatively different effects. In fact, it can be seen from Fig. 11 that, whereas at $x < 1$ the results obtained with the approximate spectral function (4.14) and with the exact one cannot practically be distinguished (cf. Fig. 5), at $x > 1$ they are totally different; it can also be seen that when the energy dependence of the spectral functions is chosen so as to describe two-nucleon correlations, the results are not very different from the exact calculation, at least up to $x \approx 1.2$. Accurate experimental data in the region $1 < x < 2$ would therefore be very useful for the investigation of the correlation structure of few-nucleon systems (see Ref. 13).

VII. SUMMARY AND CONCLUSIONS

In this paper the results of an advanced approach for the analysis of the nucleonic contribution to DIS off few-nucleon systems has been presented. The approach is based upon nuclear structure functions calculated with nucleon spectral functions resulting from accurate solutions of the few-body problem which employ realistic *NN* potentials. By this way, the strong *NN* correlations generated by the short range and tensor parts of the potential, are accurately taken into account. Our results fully confirm the finding of Ref. 19, where the EMC effect in complex nuclei has bee considered: *NN* correlations, by strongly increasing the nucleon mean removal and kinetic energies, strongly enhance the EMC effect; as a result, the experimental behavior of the ratio $R_A(x,Q^2)$ is qualitatively reproduced in the region $0.2 \leq x \leq 0.7$, provided the largely discussed flux factor which, on the contrary, reduces the EMC effect, is taken into account. For ^{4}He a comparison with the results obtained within nuclear single-particle models, has also been performed; we found, in agreement with Refs. 18 and 19, that when the flux factor is considered, these models predict only a very small EMC effect. We have also investigated the effect of Q^2 rescaling, and found only a small increase of quark confinement radius in nuclei. Eventually, the three-body structure function for $x > 1$ has been analyzed; it appears that, unlike what happens in the region $x < 1$, the behavior of the structure function for $x > 1$ is determined by the detailed correlation structure of the nucleon spectral function. In closing, the following important points, concerning the comparison between theoretical results and experimental data should be underlined:

(i) a significant comparison between theoretical results and experimental data can be performed only for ^{4}He, for experimental data on ^{3}He do not yet exist. Since theoretical calculations for three-body nuclei are the most reliable ones, experimental data on ^{3}He are urgently called for;

(ii) although from our results it can be concluded that a description in terms of nucleonic degrees of freedom which accounts for *NN* correlations is a reasonable one in the region $0.2 \leq x \leq 0.7$, it is also clear that such a description is unlikely to provide a full interpretation of the data in the whole range of x. Our results in fact, cannot reproduce, as it was *a priori* expected, the behavior of data at $x \leq 0.2$ and at the same time they are systematically larger than the experimental data at $x \approx 0.6 \div 0.7$. The explanation of both disagreements deserves careful attention and might represent a clear signature of non conventional effects.

ACKNOWLEDGMENTS

We have benefited from many discussions on different aspects of the problem with several people. We are particularly indebted to R. Arnold, L. Frankfurt, A. Krzywicki, E. Levin, E. Pace, G. Salmè and M. Strikman. We would also like to express our gratitude to K. Rith for informing us about the experimental data of the New Muon Collaboration prior to publication.

[1]W. B. Atwood and G. B. West, Phys. Rev. D 7, 773 (1973); L. L. Frankfurt and M. I. Strikman, Phys. Lett. **65B**, 51 (1976).

[2]J. J. Aubert *et al.* (European Muon Collaboration), Phys. Lett. **123B**, 275 (1983).

[3]R. G. Arnold *et al.*, Phys. Rev. Lett. **52**, 727 (1984).

[4]G. Bari *et al.* (BCDMS Collaboration), Phys. Lett. **163B**, 282 (1985).

[5]D. Nowotny, Ph.D. thesis, University of Heidelberg, 1989.

[6]A. Bodek and J. L. Ritchie, Phys. Rev. D **23**, 1071 (1981).
[7]M. Ericson and A. W. Thomas, Phys. Lett. **128B**, 112 (1983); E. L. Berger and F. Coester, Phys. Rev. D **32**, 1071 (1985).
[8]F. E. Close, R. L. Jaffe, R. G. Roberts, and G. C. Ross, Phys. Rev. D **31**, 1004 (1985).
[9]E. L. Berger and F. Coester, Annu. Rev. Nucl. Part. Sci. **37**, 463 (1987); V. Barone and E. Predazzi, Ann. Phys. (Paris) (in press).
[10]S. V. Akulinichev, S. Shlomo, S. A. Kulagin, and G. M. Vagradov, Phys. Lett. **158B**, 485 (1985); Phys. Rev. Lett. **55**, 2239 (1985).
[11]B. L. Birbrair, A. B. Gridnev, M. B. Zhalov, E. M. Levin, and V. E. Starodubski, Phys. Lett. **166B**, 119 (1986).
[12]G. V. Dunne and A. W. Thomas, Nucl. Phys. **A455**, 701 (1986).
[13](a) L. L. Frankfurt and M. I. Strikman, Phys. Lett. **183B**, 254 (1987); (b) Phys. Rep. **160**, 236 (1988).
[14]A. Krzywicki, in *Perspectives in Nuclear Physics at Intermediate Energies,* edited by S. Boffi, C. Ciofi degli Atti, and M. M. Giannini (World Scientific, Singapore, 1988) p. 159.
[15]B. L. Birbrair, E. M. Levin, and Gh. Shuvaiev, Nucl. Phys. **A491**, 618 (1989).
[16]R. L. Jaffe, Nucl. Phys. **A478**, 3c (1988).
[17]H. Jung and G. A. Miller, Phys. Lett. **B200**, 351 (1988).
[18]G. L. Li, K. F. Liu, and G. E. Brown, Phys. Lett. **B213**, 531 (1988).
[19]C. Ciofi degli Atti and S. Liuti, Phys. Lett. **B225**, 215 (1989).
[20]S. Frullani and J. Mougey, Adv. Nucl. Phys. **14**, 1 (1984).
[21]J. Le Goff *et al.* in *Proceedings of the 4th Workshop on Perspectives in Nuclear Physics at Intermediate Energies,* Trieste, 1989, edited by S. Boffi, C. Ciofi degli Atti, and M. M. Giannini (World Scientific, Singapore, 1989), p. 376.
[22]C. Ciofi degli Atti, E. Pace, and G. Salmè, Phys. Rev. C **21**, 805 (1980); Phys. Lett. **141B**, 14 (1984).
[23]T. Uchiyama and K. Saito, Phys. Rev. **38**, 2245 (1988).
[24]C. Ciofi degli Atti, Prog. Part. Nucl. Phys. **3**, 163 (1980).
[25]C. Ciofi degli Atti, E. Pace, G. Salmè, Few Body Systems **S1**, 280 (1986); Phys. Rev. C **39**, 259 (1989).
[26]D. S. Koltun, Phys. Rev. C **9**, 484 (1974).
[27]A. E. Dieperink, T. de Forest Jr., I. Sick, and R. A. Brandenburg, Phys. Lett. **63B**, 261 (1976).
[28]H. Meier-Hajduk, Ch. Hajduk, P. U. Sauer, and W. Theis, Nucl. Phys. **A395**, 332 (1983).
[29]S. Ishikawa and T. Sasakawa, Few Body Systems **1**, 143 (1986).
[30]V. R. Reid, Ann. Phys. (N.Y.) **50**, 411 (1968).
[31]Y. Akaishi, Nucl. Phys. **A463**, 127c (1987).
[32]R. Schiavilla, V. R. Pandharipande, and R. Wiringa, Nucl. Phys. **A449**, 219 (1986).
[33]M. Glück, E. Hoffman, and E. Reya, Z. Phys. C **13**, 119 (1982).
[34]A. Bodek and A. Simon, Z. Phys. C **29**, 231 (1985).
[35]U. Oelfke and P. Sauer, Czech. J. Phys. B **36**, 926 (1986).
[36]I. E. Lagaris and V. R. Pandharipande, Nucl. Phys. **A386**, 331 (1981).
[37]L. Celenza, A. Rosenthal, and C. M. Shakin, Phys. Rev. C **31**, 946 (1985); F. Guttner and H. J. Pirner, Nucl. Phys. **A457**, 555 (1986); A. W. Hendry, D. B. Lichtenberg, and E. Predazzi, Phys. Lett. **136B**, 433 (1984).
[38]I. Sick, Phys. Lett. **157B**, 13 (1985).
[39]C. Ciofi degli Atti, Nucl. Phys. **A497**, 349c (1989).
[40]I. Sick, D. B. Day, and J. S. McCarthy, Phys. Rev. Lett. **45**, 871 (1980).
[41]H. Araseki and T. Fujita, Nucl. Phys. **A439**, 681 (1985); K. Saito and T. Uchiyama, Z. Phys. A **322**, 299 (1985); S. V. Akulinichev and S. Shlomo, Phys. Rev. C **33**, 1551 (1986).
[42]C. Ciofi degli Atti, L. L. Frankfurt, S. Simula, and M. I. Strikman, in *Proceedings of the 4th Workshop on Perspectives in Nuclear Physics at Intermediate Energies, Trieste, 1989,* edited by S. Boffi, C. Ciofi degli Atti, and M. M. Giannini (World Scientific, Singapore, 1989), p. 91.
[43]J. Rozynek and M. C. Birse, Phys. Rev. C **38**, 2201 (1988).